Journal of Quantitative Spectroscopy & Radiative Transfer 122 (2013) 141–149

Contents lists available at SciVerse ScienceDirect

Journal of Quantitative Spectroscopy & Radiative Transfer

journal homepage: www.elsevier.com/locate/jqsrt

A method of retrieving cloud top height and cloud geometrical thickness with oxygen A and B bands for the Deep Space Climate Observatory (DSCOVR) mission: Radiative transfer simulations

Yuekui Yang [a,b,*], Alexander Marshak [b], Jianping Mao [b,c], Alexei Lyapustin [b], Jay Herman [b,d]

[a] Universities Space Research Association, Columbia, MD, USA
[b] NASA Goddard Space Flight Center, Greenbelt, MD, USA
[c] Earth System Science Interdisciplinary Center, University of Maryland, College Park, MD, USA
[d] Joint Center for Earth Systems Technology, UMBC, Baltimore, MD, USA

ARTICLE INFO

Article history:
Received 28 June 2012
Received in revised form
26 September 2012
Accepted 27 September 2012
Available online 11 October 2012

Keywords:
DSCOVR
L1 Lagrangian point
EPIC
Radiative transfer
Cloud top
Cloud thickness
O_2 A-band
O_2 B-band

ABSTRACT

The Earth Polychromatic Imaging Camera (EPIC) onboard the Deep Space Climate Observatory (DSCOVR) was designed to measure the atmosphere and surface properties over the whole sunlit half of the Earth from the L1 Lagrangian point. It has 10 spectral channels ranging from the UV to the near-IR, including two pairs of oxygen (O_2) A-band (779.5 and 764 nm) and B-band (680 and 687.75 nm) reference and absorption channels selected for the cloud height measurements. This paper presents the radiative transfer analysis pertinent to retrieving cloud top height and cloud geometrical thickness with EPIC A- and B-band observations. Due to photon cloud penetration, retrievals from either O_2 A- or B-band channels alone gives the corresponding cloud centroid height, which is lower than the cloud top. However, we show both the sum and the difference between the retrieved cloud centroid heights in the A and B bands are functions of cloud top height and cloud geometrical thickness. Based on this fact, the paper develops a new method to retrieve cloud top height and cloud geometrical thickness simultaneously for fully cloudy scenes over ocean surface. First, cloud centroid heights are calculated for both A and B bands using the ratios between the reflectances of the absorbing and reference channels; then the cloud top height and the cloud geometrical thickness are retrieved from the two dimensional look up tables that relate the sum and the difference between the retrieved centroid heights for A and B bands to the cloud top height and the cloud geometrical thickness. This method is applicable for clouds thicker than an optical depth of 5.

Published by Elsevier Ltd.

1. Introduction

As part of the payload of NASA's future Deep Space Climate Observatory (DSCOVR) mission, the Earth Polychromatic Imaging Camera (EPIC) was designed to observe the Earth from the L1 Lagrangian point, a gravity neutral position 1.5 million km away from the earth. At the L1 point, a satellite remains near the sun–earth line viewing the entire daytime hemisphere continuously. DSCOVR will be placed in a Lissajous Orbit about L1 providing observations of the earth at near backscatter directions with scattering angle ranging from 165° to 176°. The EPIC instrument has 10 spectral channels

* Corresponding author at: NASA Goddard Space Flight Center, Code 613, Greenbelt, MD 20771, USA.
E-mail address: Yuekui.Yang@nasa.gov (Y. Yang).

0022-4073/$ - see front matter Published by Elsevier Ltd.
http://dx.doi.org/10.1016/j.jqsrt.2012.09.017

ranging from the UV to the near-IR. As shown in Table 1, these channels will be used for measuring ozone, aerosol, cloud and vegetation properties. The pixel size of the EPIC sensor is about 8 km at nadir, but the effective instrument field of view will be larger due to the optical point-spread function. Stray light effects are corrected based on laboratory measurements [1].

Knowledge of detailed cloud information, including cloud top height and cloud optical depth for every EPIC pixel, is needed for DSCOVR to fulfill its science requirements. Among the 10 EPIC channels, two pairs of oxygen (O_2) A-band (779.5 and 764 nm) and B-band (680 and 687.75 nm) reference and absorption channels are chosen for the cloud height measurements. Fig. 1 shows the molecular oxygen absorption spectra and the selected locations of these channels. Using O_2 absorption for cloud top height retrieval was initially proposed by Yamamoto and Wark [2] based on the idea that the amount of O_2 absorption is proportional to the air mass above clouds. Since oxygen is a well-mixed gas, cloud top height can be derived from radiance measurements in the absorption band if the atmosphere is non-scattering and its vertical profile is known. This idea has been investigated extensively both in theoretical studies (e.g., Refs. [3–7]) and in operational practices (e.g., Refs. [8–12]). It has long been realized that a major uncertainty of the cloud top height retrieval with the O_2 bands comes from the multiple scattering along the photon path (e.g., Refs. [2–4,13]), which generally results in underestimation of the cloud top altitude (e.g., Refs. [14–17]). The properties of photon path length due to multiple scattering within clouds have been studied extensively in the literature (e.g., Refs. [18–22]).

This paper develops a method that employs the differences in the photon path lengths between O_2 A and B bands to retrieve cloud top height and cloud geometrical thickness simultaneously. The sensitivity of A- and B-band observations to cloud geometrical thickness comes from the wings of the absorption lines (Fig. 2). Photons at the center of an absorption line are usually absorbed. Photons at the line wings, however, can penetrate deep inside the cloud.

The remainder of the paper is organized as follows: Section 2 introduces the specifics of the EPIC O_2 A and B

Table 1
EPIC channel specifics. FWHM: full width at half maximum.

λ (nm)	Δλ (nm) FWHM	Purpose
317.5 ± 0.1	1 ± 0.2	*Ozone*
325 ± 0.1	2 ± 0.2	*Ozone*
340 ± 0.3	3 ± 0.6	*Ozone, Aerosols, Clouds*
388 ± 0.3	3 ± 0.6	*Aerosols, Clouds*
443 ± 1	3 ± 0.6	*Aerosols*
551 ± 1	3 ± 0.6	*Aerosols, Vegetation*
680 ± 0.2	2 ± 0.4	*Aerosol, Vegetation, Clouds, O_2 B-Band Reference*
687.75 ± 0.2	0.8 ± 0.2	*O_2 B-Band Cloud Height*
764.0 ± 0.2	1 ± 0.2	*O_2 A-Band Cloud Height*
779.5 ± 0.3	2 ± 0.4	*O_2 A-Band Reference, Vegetation*

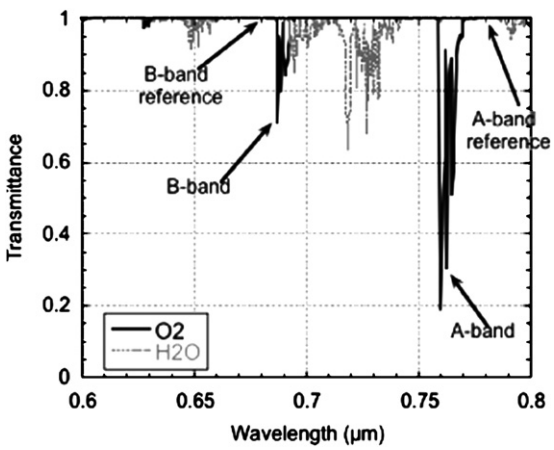

Fig. 1. Spectral locations of the EPIC oxygen A- and B-band channels. Plotted are the atmospheric transmittances due to the absorption of oxygen (solid lines) and water vapor (dotted lines). Results are from the LBLRTM model calculations.

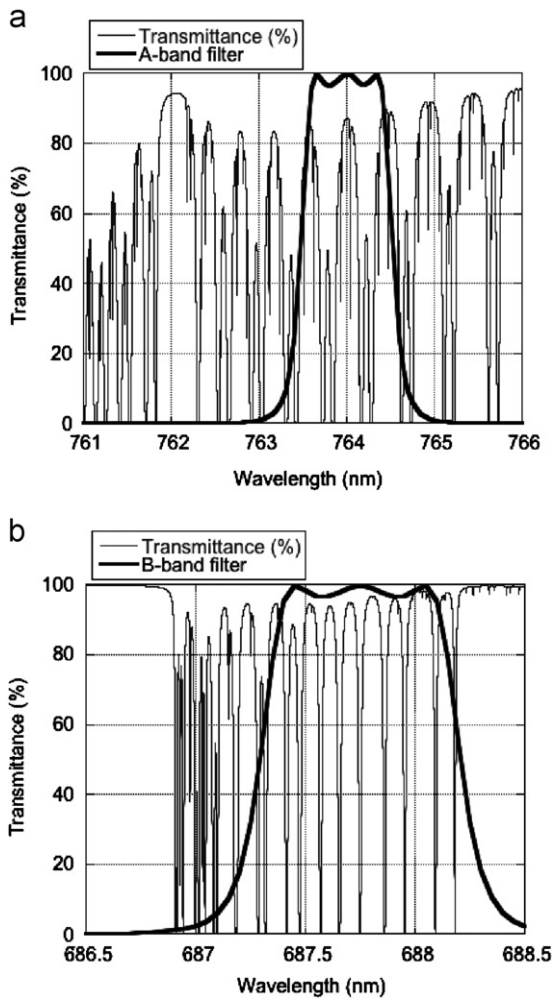

Fig. 2. EPIC A- and B-band absorption channel filter functions. Also plotted are the atmospheric transmittances calculated with the LBLRTM model. (a) A-band; (b) B-band.

bands; Section 3 describes the two commonly used cloud height retrieval methods with O_2 bands and their relationships; in Section 4, the differences between A- and B-band retrievals are discussed; the approach of retrieving cloud top height and cloud geometrical thickness is described in Section 5; and the results are summarized in Section 6.

2. EPIC oxygen A and B bands

Fig. 2 shows the EPIC A- and B-band filter functions along with the high-resolution O_2 absorption spectra. For the O_2 A-band, the full width at half maximum (FWHM) is 1 nm with an uncertainty about 0.2 nm; for the O_2 B-band the FWHM is 0.8 nm with a similar uncertainty. Unless otherwise noted, all the radiative transfer simulations on O_2 absorption conducted in this paper are based on these filter functions. The Discrete Ordinates Radiative Transfer model (DISORT) [23] is adopted for the calculations. The optical properties of the cloudy atmosphere were calculated with the Line-By-Line Radiative Transfer Model (LBLRTM) [24] for the 1976 U.S. standard atmosphere [25] and monochromatic radiative transfer results were convoluted with the filter functions.

The O_2 A- and B-band radiances registered at the EPIC sensor will be the result of a complex radiative transfer process. For the convenience of our discussion, we denote the distance from the sun to the cloud top and then to the satellite detector as $\boldsymbol{l_{ct}}$. It represents an ideal measurement for a fully cloudy pixel in the absence of photon cloud penetration and the above-cloud reflectance. In this case, the monochromatic radiance at the top of the atmosphere (TOA) can be directly related to $\boldsymbol{l_{ct}}$ via Beer's law; hence cloud top height retrieval with the O_2 bands would be trivial. In reality, however, photon paths can be very complicated. Fig. 3 illustrates different pathways for a photon reflected by the atmosphere–surface system reaching the sensor. Shown in the figure is a single pixel with partial cloud cover. A photon can come from any of the six depicted pathways and may experience multiple scattering along its path. The six pathways include photons: (1) reflected by the Rayleigh layer below the cloud; (2) reflected by the Rayleigh layer above the cloud; (3) reflected by the cloud layer; (4) reflected by the surface below the cloud; (5) reflected by the Rayleigh layer on the clear side of the pixel; and (6) reflected by the surface on the clear side of the pixel. Here, the pathways are defined by the deepest point that the photon reaches whereas interactions inside and between the layers are included in the photon pathways. Obviously, when the pixel is fully cloudy, Path 5 and 6 do not exist. For thick clouds, the contribution of photons that follow Path 1 and Path 4 is negligible. When all pathways are present, compared to $\boldsymbol{l_{ct}}$, the photon path lengths associated with Path 1, 3, 4 and 6 are usually longer, hence corresponding to larger O_2 absorption. Path 2 is shorter, hence corresponding to smaller absorption. Path 2 represents the Rayleigh reflectance above cloud. Even though the Rayleigh optical depths at the O_2 A- and B-band wavelengths are small, their effects on cloud height retrieval are significant. As demonstrated by Wang et al. [26], who showed that accounting for Rayleigh scattering at A-band leads to about a 50 hPa difference in pressure retrieval globally. For B-band the effect is expected to be significantly larger.

Even though the complexity of the photon pathways makes the cloud property retrieval a challenging task, critical information can be obtained with EPIC O_2 channels. As an example, Fig. 4 shows the ratios between the absorption channel and the reference channel radiances for both EPIC A and B bands as a function of cloud top height for a variety of cloud optical depths (COD). For a given cloud thickness, cloud optical properties and surface albedo, the ratios are monotonic functions of cloud top height. The ratios for optically thin clouds (the COD = 1 line) demonstrate a smaller sensitivity to cloud altitude compared to optically thick clouds. This is due to the relative importance

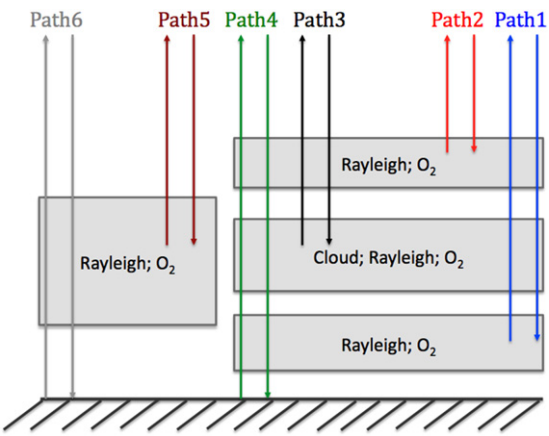

Fig. 3. Basic pathways for a photon to reach the sensor. Shown is one EPIC pixel with partial cloud coverage.

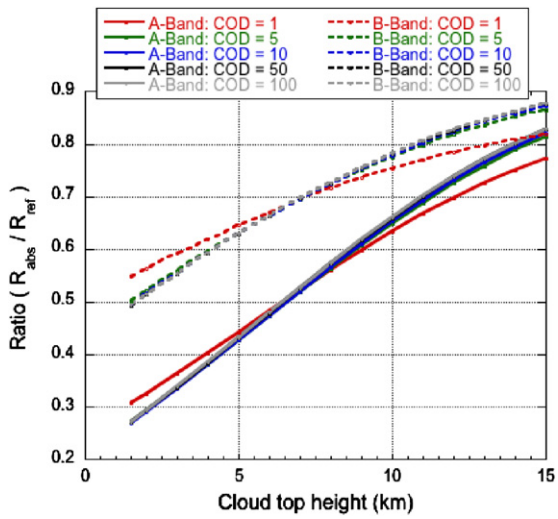

Fig. 4. Ratios of the absorption (R_{abs}) and the reference (R_{ref}) channel reflectances for both the EPIC O_2 A (solid lines) and B (dashed lines) bands as a function of cloud top height. Surface is assumed black; and cloud thickness is 1 km. Mie phase function with an effective radius of 10 μm is used. Solar zenith angle (SZA) = Viewing zenith angle (VZA) = 40°. The relative azimuth angle (RAA) = 172°.

of Rayleigh scattering: for low clouds, Rayleigh scattering happens mostly above clouds (Path 2 in Fig. 3), resulting in a shorter average photon path and hence a smaller O_2 absorption. Since the reference channel reflectances are not affected by photon path lengths, a shorter average photon path will correspond to an increased ratio value; for high clouds, since the cloud is optically thin, the contribution of the Rayleigh layer below the cloud increases (Path 1 in Fig. 3), resulting a longer average photon path and a decreased ratio value. Obviously, the effect of Rayleigh scattering is larger in the B-band than in the A-band.

Since the TOA radiances of the O_2 channels are a function of several parameters, including cloud thickness, cloud microphysics and surface albedo (e.g., Ref. [3,8]), it is challenging to retrieve the cloud top height with one pair of the EPIC O_2 band channels. However, as will be demonstrated later, the differences in A- and B-band absorption contains information about cloud thickness and with some limitations, cloud thickness and cloud top height can be simultaneously retrieved through a combination of O_2 A- and B-band observations.

3. Two basic methods for cloud height retrieval

This section discusses two commonly used cloud height retrieval methods with the O_2 bands, the mixed Lambertian-equivalent reflectivity (MLER) method and the ratio method. Since neither method considers photon cloud penetration, both retrieve a cloud height that is lower than the cloud top. To distinguish the cloud heights retrieved with these two methods from the actual cloud top height, we call them the cloud centroid heights (and the corresponding pressures the cloud centroid pressures) following Joiner et al. [29].

3.1. The MLER method

Given the complexity of the photon paths, simplifications and assumptions are needed in order to retrieve cloud height with an oxygen band. The MLER model has been extensively studied and applied in the operational practices (e.g., Refs. [8,15,17,26,27]). It assumes that the pixel contains two Lambertian reflectors, the surface and the cloud. The cloud is assumed opaque, hence no photon transmission through clouds. The reflectance observed at the sensor can be expressed as

$$R_{abs}(\theta,\theta_0) = (1-A_c)\alpha_s T_{abs}(P_s,\theta,\theta_0) + A_c\alpha_c T_{abs}(P_c,\theta,\theta_0) \quad (1)$$

$$R_{ref}(\theta,\theta_0) = (1-A_c)\alpha_s T_{ref}(P_s,\theta,\theta_0) + A_c\alpha_c T_{ref}(P_c,\theta,\theta_0) \quad (2)$$

where R_{abs} and R_{ref} are the observed bidirectional reflectances for the absorption and the reference channels, A_c is the cloud fraction, α_s is the surface albedo, α_c is the cloud reflectance, T_{abs} and T_{ref} are the two-way transmittances for the absorption and the reference channels, P_c and P_s are the cloud centroid pressure and the surface pressure, and θ and θ_0 are the view zenith and solar zenith angles, respectively. Since it is generally not feasible to derive cloud fraction and cloud optical thickness independently with one oxygen band, the MLER model assumes a cloud reflectance of 0.8 and A_c is derived as the effective cloud fraction. A reflectance of 0.8 corresponds to an optically thick cloud. This value is selected to justify the no transmission assumption of the MLER model. It has been demonstrated that although the selection of cloud reflectance value clearly affects the results of the effective cloud fraction, its effect on the retrieved cloud centroid pressure is small [8,27]. Note that when a cloud is thick enough with albedo exceeding 0.8 the effective cloud fraction can be larger than one.

Cloud centroid pressure can be retrieved with Eqs. (1) and (2) through iteration. This value can then be converted to cloud centroid height according to the atmospheric profile. As mentioned in Section 2, the EPIC reflectances used in this study are simulated with DISORT with input from the LBLRTM model.

3.2. The ratio method

Another way of retrieving cloud height is to use the ratio between the absorption channel and the reference channel reflectances [4,12,14]. Assuming that a pixel is fully cloudy and there is no light transmission through the cloud, we have:

$$\frac{T_{abs}(P_c,\theta,\theta_0)}{T_{ref}(P_c,\theta,\theta_0)} = \frac{R_{abs}(\theta,\theta_0)}{R_{ref}(\theta,\theta_0)} \quad (3)$$

Since T_{abs} and T_{ref} for each layer are pre-calculated, retrieving cloud centroid pressure (P_c) with this method is straightforward. First, a look up table of the ratios of T_{abs} and T_{ref} (left hand side of Eq. (3)) is generated. Then for each pair of R_{abs} and R_{ref}, P_c can be found by searching the look up table. Similar to the MLER, the ratio method does not consider light penetration into and through the cloud; hence the retrieved cloud altitude (the centroid height) is also lower than the cloud top. The land surface reflectance, which is usually high in the near-IR region and is not accounted for in Eq. (3), is another factor that affects the retrieval, especially when clouds are thin. Correction schemes have been developed to take these effects into account [12,14].

Based on the above description, two EPIC cloud centroid heights can be obtained for each method based on A-band and B-band pairs of measurements.

3.3. Relationship between the retrievals of the two methods

To further understand the retrievals from the two methods, we combine Eqs. (1) and (2) of the MLER method to obtain:

$$\frac{T_{abs}(P_c,\theta,\theta_0)}{T_{ref}(P_c,\theta,\theta_0)} = \frac{R_{abs}(\theta,\theta_0)-(1-A_c)\alpha_s T_{abs}(P_s,\theta,\theta_0)}{R_{ref}(\theta,\theta_0)-(1-A_c)\alpha_s T_{ref}(P_s,\theta,\theta_0)} \quad (4)$$

With Eq. (4), the cloud height can then be retrieved using the same look up table as the ratio method as long as the effective cloud fraction A_c is determined. As shown in Fig. 4, the larger the ratio between $T_{abs}(P_c, \theta, \theta_0)$ and $T_{ref}(P_c, \theta, \theta_0)$, the higher the retrieved cloud height.

Let us denote the value of $\frac{T_{abs}(P_c,\theta,\theta_0)}{T_{ref}(P_c,\theta,\theta_0)}$ derived from the ratio method (Eq. (3)) as r_{ratio}, and the one from the MLER method (Eq. (4)) as r_{MLER}. The corresponding retrieved cloud centroid height from the ratio method will be referred to as h_{ratio} and the one from the MLER method h_{MLER}, respectively. By comparing Eq. (3) and Eq. (4), it is

easy to see that when $A_c=1$, or $\alpha_s=0$ (black surface), the two methods give the same results. Also, the two methods would be equivalent if the following relationship held true:

$$\frac{T_{abs}(P_s,\theta,\theta_0)}{T_{ref}(P_s,\theta,\theta_0)}=\frac{R_{abs}(\theta,\theta_0)}{R_{ref}(\theta,\theta_0)} \tag{5}$$

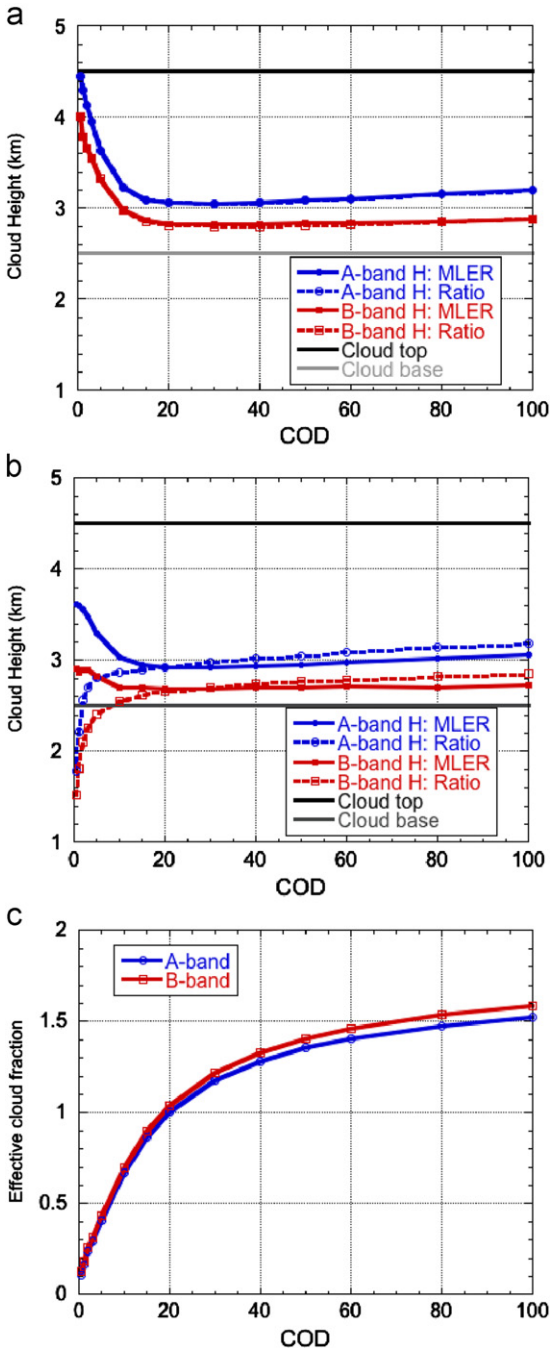

Fig. 5. (a) Comparisons of retrievals from the MLER method and the ratio method for black surface; (b) same as (a), but for surface albedo 0.1; (c) cloud effective fraction from the MLER model corresponding to the case shown in (b). Mie phase function for an effective radius of 10 μm is used. Clouds are located between 2.5 km and 4.5 km. The solar zenith and view zenith angles are both assumed to be 0°.

In reality, however, most cases follow the rule,

$$\frac{T_{abs}(P_s,\theta,\theta_0)}{T_{ref}(P_s,\theta,\theta_0)}<\frac{R_{abs}(\theta,\theta_0)}{R_{ref}(\theta,\theta_0)} \tag{6}$$

because generally the path lengths of photons reflected by the surface is longer than those reflected by the clouds. Hence for realistic surface ($\alpha_s>0$), depending on the sign of $(1-A_c)$, the retrieved h_{ratio} can be either larger or smaller than h_{MLER}: if $A_c>1$ (thick clouds with albedo >0.8), then $r_{ratio}>r_{MLER}$ and $h_{ratio}>h_{MLER}$. In this case, the ratio method gives higher cloud centroid height. On the contrary, if $A_c<1$ (thinner clouds), then $r_{ratio}<r_{MLER}$ and $h_{ratio}<h_{MLER}$, so that the ratio method gives lower cloud centroid height. Fig. 5 shows an illustration of the discussed cases. For example, Fig. 5a shows that the two methods give the same results for a black surface. Over a reflecting surface, however, as discussed above, the ratio method gives lower retrievals when the effective cloud fraction A_c is smaller than 1 and gives higher retrievals when $A_c>1$ (Fig. 5b and c). Note that as a result of using only one absorption channel and one reference channel, the cloud centroid heights retrieved with both methods are considerably lower than the cloud top. These results are consistent with previous studies (e.g., Refs. [13–17]). Since Eqs. (1) and (2) have included the contribution of surface, the retrievals from the MLER model is less affected by the surface albedo compared to the ratio method.

4. Differences in EPIC oxygen A- and B-band retrievals

Due to different absorption and different effective depth of light penetration into a cloud, the cloud centroid height retrieved from the O_2 B-band is generally lower than that from the A-band regardless of the retrieval method used. This phenomenon is illustrated in Fig. 5a and b, which also shows that the differences between O_2 A- and B-band retrievals for the two methods are very close to each other. In the following discussions, we will use the cloud centroid heights retrieved with the ratio method.

For clarity, let us denote the cloud centroid heights retrieved from the O_2 A and B bands as h_A and h_B, and the difference between them as h_{diff}. Fig. 6 shows h_A and h_B as a function of EPIC sun-view geometry. For this case, clouds are located between 2 and 4 km. The difference h_{diff} is mainly caused by the different absorption strengths of O_2 A and B bands. The stronger absorption of A-band results in a shorter total path length and shallower apparent cloud penetration depth [28]. Hence h_{diff} is generally positive. Fig. 6 shows that h_{diff} decreases with increase of solar and view zenith angles, which is caused by the increasing contribution from the Rayleigh layer above the cloud (Path 2 in Fig. 3) [26]. As mentioned before, compared to the photons reflected by the cloud, photons through Path 2 act to decrease the average photon path length resulting a higher retrieval in the centroid cloud height. This effect is larger in the B-band than in the A-band. As shown in Fig. 7a (the COD=5 line), if the effect is strong enough, the cloud centroid height

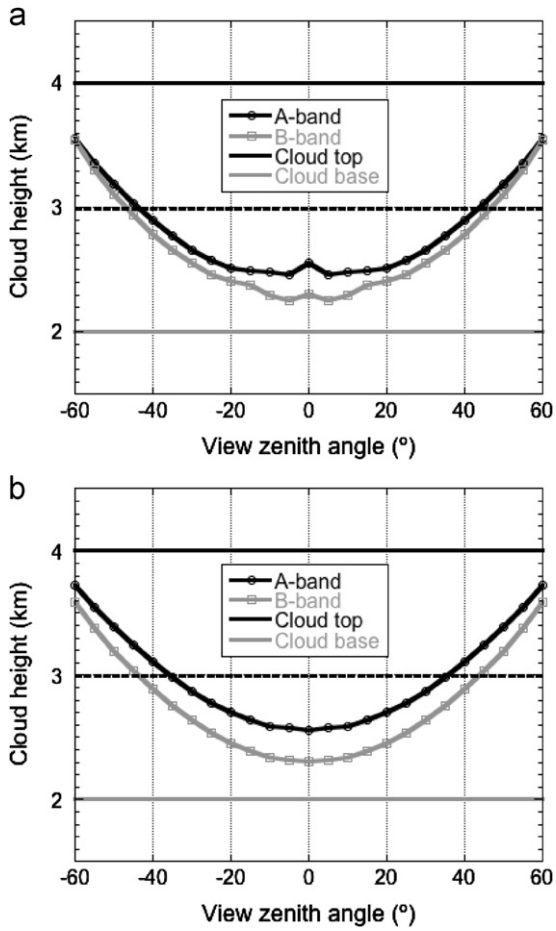

Fig. 6. Comparison of A-band and B-band retrievals under DSCOVR sun-view geometry (SZA=VZA). Surface is assumed black; hence the MLER method and the ratio method give the same results. The dashed line gives the center altitude of the cloud. Clouds are located between 2 km and 4 km. Cloud optical depth are assumed to be 30. (a) RAZ=172°; (b) RAZ=180°.

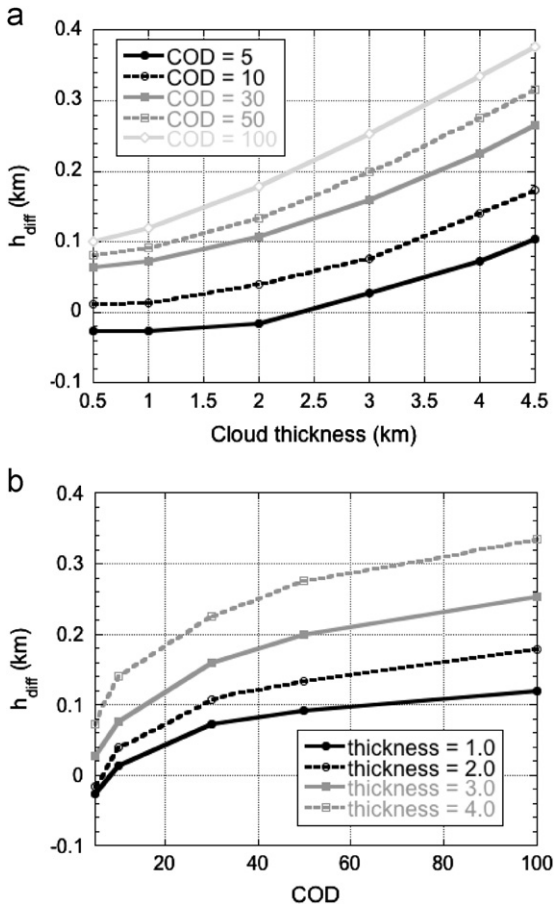

Fig. 7. The cloud centroid height differences between A-band and B-band retrievals (h_{diff}) (a) as a function of cloud thickness for a variety of cloud optical depths and (b) as a function of cloud optical depth for a variety of cloud thicknesses. Simulations are for dark surface; SZA=VZA=40°; RAZ=172°; cloud top height=5 km.

retrieved from the B-band can be higher than that from the A-band and h_{diff} can be negative.

The retrieved cloud centroid heights from the O_2 bands are not only a function of the cloud top altitude, but also a function of cloud geometrical thickness. Fig. 7a and b illustrate this point. For the cases displayed in Fig. 7, h_{diff} increases with both the increase of cloud geometrical thickness and the increase of cloud optical thickness. This can be explained by looking at the photon path length difference between A and B bands. Denote l_{total} as the total photon path length inside the cloud layer, then

$$l_{total} = \langle n_R \rangle l_{free} \tag{7}$$

where $\langle n_R \rangle$ is the average number of scattering inside a cloud experienced by a reflected photon and l_{free} is the mean free path inside the cloud:

$$l_{free} = \frac{H}{\tau_{cld} + \tau_{Rayleigh} + \tau_{O_2}} \tag{8}$$

where τ_{cld} is the cloud optical depth and $\tau_{Rayleigh}$ and τ_{O_2} are the optical depths of Rayleigh and Oxygen within the cloud layer respectively. Theoretically, since τ_{O_2} is different for A- and B-band, l_{free} is also different for the two bands. However, the equivalent EPIC band averaged O_2 optical depths (~0.6 for A band and ~0.3 for B band) is very small compared to the COD considered here (from 5 to 100); hence as an approximation, l_{free} can be considered the same for EPIC A and B bands.

In the diffusion regime, $\langle n_R \rangle$ can be expressed as [28]

$$\langle n_R \rangle = \sigma L_d \frac{6\chi}{\kappa_+^2 e^{H/L_d} - \kappa_-^2 e^{-H/L_d}} \left(\kappa_+ e^{H/L_d} + \kappa_- e^{-H/L_d} - 2 \right) \tag{9}$$

where $\sigma = \frac{\tau_{cld} + \tau_{Rayleigh} + \tau_{O_2}}{H}$ is the extinction coefficient, χ is the extrapolation length and can be set as 0.5, $L_d = \frac{1}{\sigma\sqrt{3(1-\omega_0)(1-\omega_0 g)}}$ is the characteristic diffusion length scale (g is the asymmetry factor and $\omega_0 = \frac{\tau_{cld} + \tau_{Rayleigh}}{\tau_{cld} + \tau_{Rayleigh} + \tau_{O_2}}$ is the single scattering albedo) and $k_\pm = 1 \pm \chi\sqrt{\frac{3(1-\omega_0)}{(1-\omega_0 g)}}$.

Fig. 8 gives the results calculated from Eqs. (7)–(9). For the COD range considered here, $\langle n_R \rangle$ increases with COD but decreases with cloud geometrical thickness H

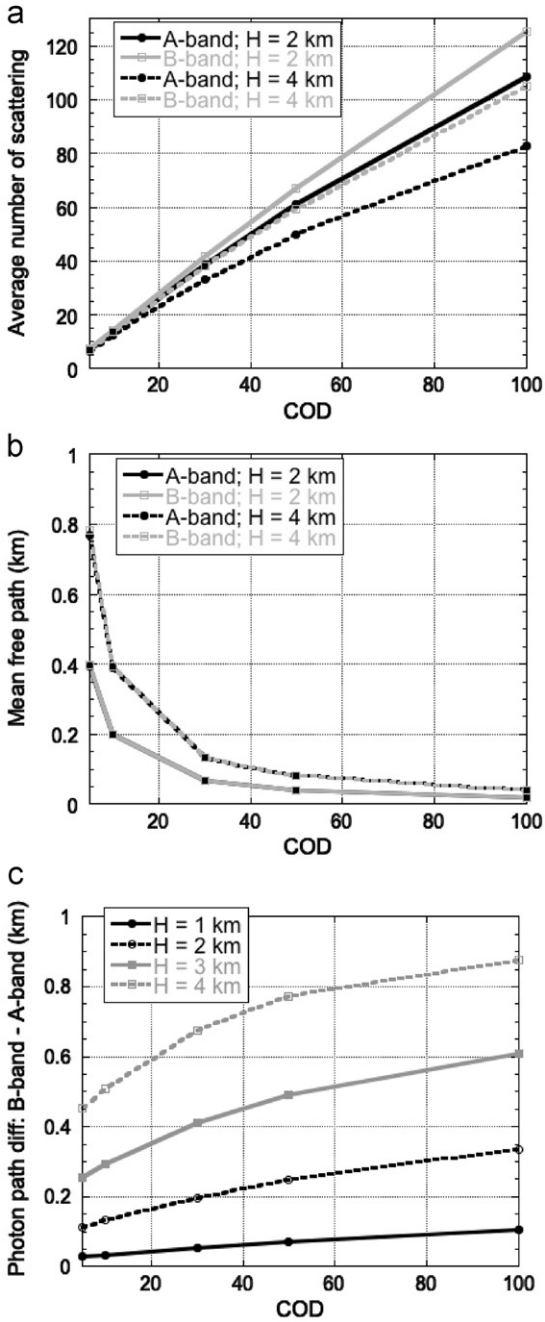

Fig. 8. (a) Average number of scattering experienced by backscattered photons inside a cloud (calculations based on Eq. (9)). H is cloud geometrical thickness; (b) photon mean free paths as a function of COD; (c) total photon paths difference between A- and B-band. Cloud top height is 5 km.

(Fig. 8a); photon mean free path decreases with COD but increases with H (Fig. 8b). Fig. 8b also shows that for the same cloud, photon mean free paths for A- and B-band are essentially the same. As shown in Fig. 8c, the end result is that the total photon path differences between A- and B-band increase with both COD and cloud geometrical thickness. Since the total photon path difference between A- and B-band is directly proportional to h_{diff}, hence h_{diff} also increases as COD and cloud thickness increas as observed in Fig. 7a and b.

5. Simultaneous retrieval of cloud top height and cloud geometrical thickness

For a given sun-view geometry and atmospheric temperature and pressure profile, the TOA radiance in the O_2 bands is a function of multiple parameters, including cloud top height, optical and geometrical thickness, particle size and shape, cloud fraction, surface albedo and aerosol loading. Among these factors, the effect of cloud particle size and shape is small (e.g., Ref. [28]). Surface albedo is important for thin clouds, but for thick clouds its contribution is limited. In this study, we focus on the ocean surface and assume a surface albedo of 0.05. While EPIC will also be used to make aerosol retrievals, this study neglects aerosol effect. We will further assume that cloud fraction equals to one for cloudy pixels, and cloud optical depth is known. In this case, radiances in O_2 absorbing bands mainly depend on cloud top height and cloud geometrical thickness, which can be evaluated using EPIC combined A and B-band observations. This procedure is described next.

Two sets of look up tables are generated for the algorithm. The first set (LUT-1) is for the retrieval of A-band and B-band cloud centroid heights with the ratio method. This set of look up tables relates the ratios between the radiances in the EPIC O_2 A and B bands and their reference channels to the A-band and B-band cloud centroid heights, h_A and h_B. After h_A and h_B are retrieved based on LUT-1, the quantities h_{sum} and h_{diff} are calculated as:

$$h_{sum} = h_A + h_B \tag{10}$$

$$h_{diff} = h_A - h_B \tag{11}$$

Both h_{sum} and h_{diff} are functions of cloud top height and geometrical thickness. Examples of this dependence are given in Fig. 9 for different values of cloud optical depth. Panel (a) shows the case for an optically thick cloud with COD = 30. In this case, one can observe a near orthogonal behavior with h_{diff} primarily depending on cloud thickness and h_{sum} depending on cloud top height. This figure shows that h_{diff} slightly decreases with the cloud top height. This decrease can be explained by the lower air density at higher altitudes, which reduces the difference in the photon's path length in the cloud between the A and B bands, as compared to the lower altitudes in the atmosphere.

Fig. 9b is the h_{sum} vs. h_{diff} diagram for COD = 10. In this case, the effect of the Rayleigh layer above the cloud matters. As discussed, compared to the photons reflected by the cloud, photons reflected by this Rayleigh layer have a shorter path length and this effect is much stronger for B-band than for A-band. The lower the cloud, the thicker the above-cloud Rayleigh layer; hence h_{diff} decreases as clouds become lower (Fig. 9b and c). When cloud is optically thin, the Rayleigh effect can result in a much less sensitivity of h_{diff} on cloud thickness and accurate retrievals become difficult (Fig. 9c). One way of dealing

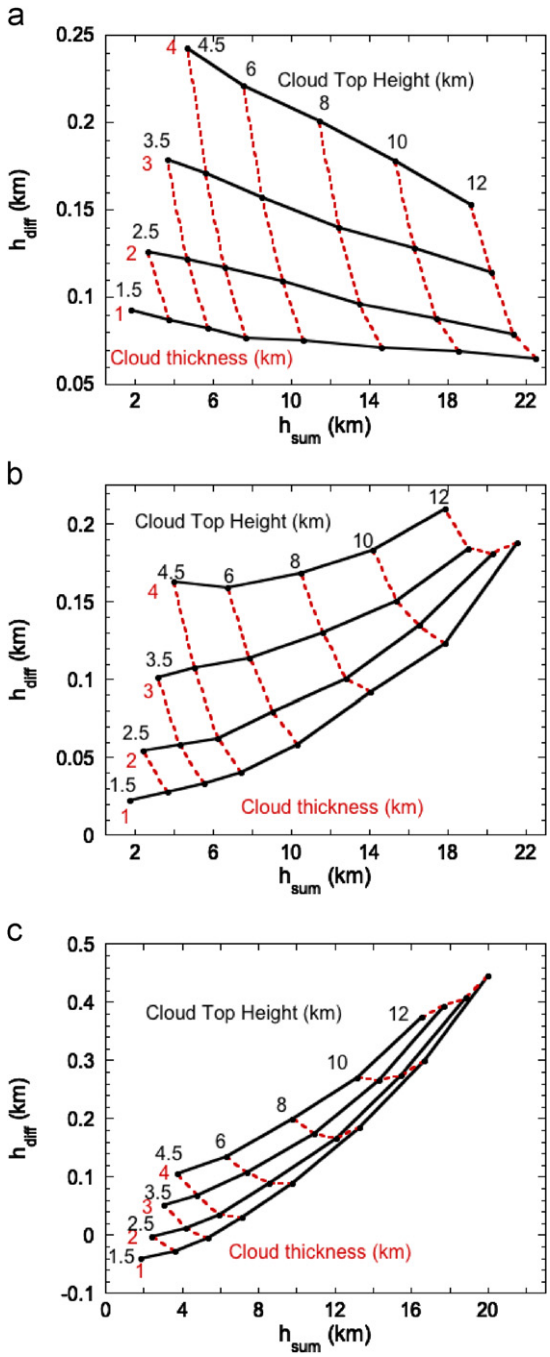

Fig. 9. Look up tables for retrieving cloud top height and cloud geometrical thickness simuteniously with EPIC oxygen bands. SZA=VZA=40°; RAZ=172°; surface albedo=0.05; Mie phase function with efective radius=10 μm. (a) COD=30; (b) COD=10; and (c) COD=5.

with this problem is to correct the Rayleigh effect as described in Wang et al. [26].

Based on the analysis of Fig. 9, the second set of look up tables (LUT-2) is generated to relate h_{sum} and h_{diff} to cloud top height and cloud geometrical thickness for a representative set of cloud optical depth for the DSCOVR view geometry. With LUT-1 and LUT-2, the retrieval process is straightforward. First, h_A and h_B are retrieved based on LUT-1; then h_{sum} and h_{diff} are calculated (Eqs. (10) and (11)); third, for a given COD, EPIC cloud top height and cloud geometrical thickness can be retrieved simultaneously by searching LUT-2.

We note that the method presented here does not consider partially cloudy cases and the radiative transfer calculations conducted in this study did not take into account the possible differences between A- and B-band surface albedo over land; hence the method works best over ocean surfaces. Over land, surface related corrections are needed.

This paper does not consider the effect of broken cloudiness and assumes that all cloudy pixels are fully covered by clouds. Recently, Linstrot et al. [30] studied the effect of sub-pixel variability in $10\times10\,km^2$ pixels on cloud height retrievals. Based on the Medium Spectral Resolution Imaging Spectrometer (MERIS) high spatial resolution O_2 A-band ($1\times1\,km^2$) data they found that fully cloudy pixels are only weakly affected by coarser spatial resolution while for broken cloud fields there is a bias towards more middle atmosphere clouds: high clouds are retrieved lower and low clouds higher.

It should be emphasized that even though the two basic approaches presented in Section 3 do not account for the photon penetration, efforts have been made in previous studies to tackle the problem. For example, the work by Wu [13] systematically studied the effect of photon penetration on cloud height retrieval with the O_2 A-band. Utilizing one off-band channel and two in-band channels, Wu showed that both the cloud top height and the scaled absorption coefficient could be retrieved. Other examples of retrieving true cloud top heights instead of centroid heights include Fischer and Grassl [3], Kokhanovsky et al. [9], Stephens and Heidinger [6], Daniel et al. [7] etc.

6. Summary and discussions

The EPIC instrument onboard DSCOVR was designed to observe the entire daytime hemisphere of the earth continuously from the L1 Lagrangian point. Retrieval of cloud properties is an important part of the science goal of the mission. This paper presents a new method of retrieving cloud top height and cloud geometrical thickness with the EPIC O_2 A- and B-band observations. Major results can be summarized as follows:

1) Two commonly used cloud height retrieval methods, the MLER method and the ratio method, are examined. Generally, when applied to O_2 A- or B-band observations, both methods retrieve a cloud centroid height that is lower than the cloud top. The MLER method assumes a constant cloud reflectance of 0.8 and thus it may retrieve an effective cloud fraction A_c larger than 1.0. For black surface or if $A_c=1.0$, the centroid height retrievals from two methods are the same; if $A_c>1.0$ (optically thick clouds), then the ratio method gives a higher cloud centroid height and vice versa for $A_c<1.0$ (optically thin clouds).

2) Differences between the A-band and B-band cloud centroid heights contain an additional piece of information on cloud geometrical thickness. We have demonstrated that with the h_{sum} vs. h_{diff} method, which combines the EPIC A- and B-band results, the cloud top height and cloud geometrical thickness can be retrieved simultaneously. This method requires knowledge of COD. The COD information can be independently derived from EPIC measurements in the non-absorbing channels. The h_{sum} vs. h_{diff} method shows promise for clouds with an optical depth larger than 5. For clouds with optical depth smaller than 5, Rayleigh correction is needed before the method can be applied.

Acknowledgments

We thank two anonymous reviewers for reviewing this manuscript and for their insightful comments. This study is supported by the NASA DSCOVR refurbishement project.

References

[1] Cede A, Mobilia J, Demroff H, Sawyer K, Hertzberg E, Herman JR. Stray light in EPIC. American Geophysical Union fall meeting. San Francisco, CA: USA; 2011.
[2] Yamamoto G, Wark D. Discussion of the letter by R. A. Hanel: determination of cloud altitude from a satellite. J Geophys Res 1961;66:3569.
[3] Fischer J, Grassl H. Detection of cloud-top height from backscattered radiances within the oxygen A band. Part I: theoretical study. J Appl Meteorol 1991;30:1245–59.
[4] O'Brien DM, Mitchell RM. Error estimates for retrieval of cloud-top pressure using absorption in the A band of oxygen. J Appl Meteorol 1992;31:1179–92.
[5] Kuze A, Chance KV. Analysis of cloud top height and cloud coverage from satellites using the O_2 A and B bands. J Geophys Res 1994;99: 14481–92.
[6] Stephens GL, Heidinger AK. Molecular line absorption in a scattering atmosphere: Part I. Theory. J Atmos Sci 2000;57:1599–614.
[7] Daniel JS, Solomon S, Miller HL, Langford AO, Portmann RW, Eubank CS. Retrieving cloud information from passive measurements of solar radiation absorbed by molecular oxygen and O_2–O_2. J Geophys Res 2003;108:4515. http://dx.doi.org/10.1029/2002JD002994.
[8] Koelemeijer RBA, Stammes P, Hovenier JW, de Haan JF. A fast method for retrieval of cloud parameters using oxygen A band measurements from the Global Ozone Monitoring Experiment. J Geophys Res 2001;106:3475–90.
[9] Kokhanovsky AA, Rozanov VV, Burrows JP, Eichmann K-U, Lotz W, Vountas M. The SCIAMACHY cloud products: algorithms and examples from ENVISAT. Adv Space Res 2005;36:789–99, http://dx.doi.org/10.1016/j.asr.2005.03.026.
[10] Preusker R, Lindstrot R. Remote sensing of cloud-top pressure using moderately resolved measurements within the oxygen A band—a sensitivity study. J Appl Meteorol Climatol 2009;48:1562–74, http://dx.doi.org/10.1175/2009JAMC2074.1.
[11] Lindstrot R, Preusker R, Ruhtz T, Heese B, Wiegner M, Lindemann C, et al. Validation of MERIS cloud top pressure using airborne lidar measurements. J Appl Meteorol Climatol 2006;45:1612–21.
[12] Buriez J-C, Vanbauce C, Parol F, Goloub P, Herman M, Bonnel B, et al. Cloud detection and derivation of cloud properties from POLDER. Int J Remote Sensing 1997;18:2785–813.
[13] Wu M-LC. Remote sensing of cloud-top pressure using reflected solar radiation in the oxygen A-band. J Clim Appl Meteorol 1985;24:539–46.
[14] Vanbauce C, Cadet B, Marchand RT. Comparison of POLDER apparent and corrected oxygen pressure to ARM/MMCR cloud boundary pressures. Geophys Res Lett 2003;30(5): 1212. http://dx.doi.org/10.1029/2002GL016449.
[15] Sneep M, de Haan JF, Stammes P, Wang P, Vanbauce C, Joiner J, et al. Three-way comparison between OMI and PARASOL cloud pressure products. J Geophys Res 2008;113:D15S23, http://dx.doi.org/10.1029/2007JD008694.
[16] Ferlay N, Thieuleux F, Cornet C, Davis AB. Toward new inferences about cloud structures from multidirectional measurements in the oxygen A band: middle-of-cloud pressure and cloud geometrical thickness from POLDER-3/PARASOL. J Appl Meteorol Climatol 2010;49:2492–507. http://dx.doi.org/10.1175/2010JAMC2550.1.
[17] Vasilkov A, Joiner J, Spurr R, Bhartia PK, Levelt P, Stephens G. Evaluation of the OMI cloud pressures derived from rotational Raman scattering by comparisons with other satellite data and radiative transfer simulations. J Geophys Res 2008;113: D15S19. http://dx.doi.org/10.1029/2007JD008689.
[18] Marshak A, Davis A, Wiscombe W, Cahalan RF. Radiative smoothing in fractal clouds. J Geophys Res 1995;100:26247–61.
[19] Davis AB, Polonsky IN, Marshak A. Space–time Green functions for diffusive radiation transport. Application to active and passive cloud probing. In: Kokhanovsky AA, editor. Light scattering reviews, vol. 4. Spring-Verlag, New York; 2009. p. 169–292.
[20] Min QL, Harrison LC. Joint statistics of photon path length and cloud optical depth. Geophys Res Lett 1999;26:1425–8.
[21] Min QL, Harrison LC, Kiedron P, Berndt J, Joseph E. A high-resolution oxygen A-band and water vapor band spectrometer. J Geophys Res 2004;109:D02202. http://dx.doi.org/10.1029/2003JD003540.
[22] Yang Y, Marshak A, Varnai T, Wiscombe W, Yang P. Uncertainties in ice-sheet altimetry from a spaceborne 1064-nm single-channel lidar due to undetected thin clouds. IEEE Trans Geosci Remote Sensing 2010;48:250–9.
[23] Stamnes K, Tsay S–C, Wiscombe WJ, Jayaweera K. Numerically stable algorithm for discrete-ordinate-method radiative transfer in multiple scattering and emitting layered media. Appl Opt 1988;27: 2502–12.
[24] Clough SA, Shephard MW, Mlawer EJ, Delamere JS, Iacono MJ, Cady-Pereira K, et al. A summary of the AER codes, short communication. J Quant Spectrosc Radiat Transfer 2005;91:233–44.
[25] U.S. standard atmosphere. Washington, D.C.: U.S. Government Printing Office; 1976.
[26] Wang P, Stammes P, van der A. R, Pinardi G, van Roozendael M. FRESCO+: an improved O_2 A-band cloud retrieval algorithm for tropospheric trace gas retrievals. Atmos Chem Phys 2008;8: 6565–76.
[27] Stammes P, Sneep M, de Haan JF, Veefkind JP, Wang P, Levelt PF. Effective cloud fractions from the Ozone Monitoring Instrument: theoretical framework and validation. J Geophys Res 2008;113: D16S38. http://dx.doi.org/10.1029/2007JD008820.
[28] Marshak A, Davis A. 3D radiative transfer in cloudy atmospheres. Springer, New York; 2005. [p. 543–86].
[29] Joiner J, Vasilkov AP, Bhartia PK, Wind G, Platnick S, Menzel WP. Detection of multi-layer and vertically-extended clouds using A-train sensors. Atmos Meas Tech 2010;3:233–47, http://dx.doi.org/10.5194/amt-3-233-2010.
[30] Lindstrot R, Bernartz R, Preuske R, Fischer J. The impact of subscale inhomogeneity on oxygen A-band cloud-top pressure estimates: using ESA's MERIS as a proxy for DSCOVR-EPIC. Remote Sensing 2012;4:1963–73.